Reconfigurable Intelligent Surface Empowered Underlaying Device-to-Device Communication

Gang Yang*, *Member, IEEE*, Yating Liao*, Ying-Chang Liang*, *Fellow, IEEE*, and Olav Tirkkonen†
*University of Electronic Science and Technology of China, Chengdu, P. R. China
†Aalto University, Aalto, Finland
Email: yanggang@uestc.edu.cn, 2015010913035@std.uestc.edu.cn, liangyc@ieee.org, olav.tirkkonen@aalto.fi

***Abstract*—Reconfigurable intelligent surfaces (RIS) are a new and revolutionary technology to achieve spectrum-, energy- and cost-efficient wireless networks. This paper studies the resource allocation for RIS-empowered device-to-device (D2D) communication underlaying a cellular network, in which an RIS is employed to enhance desired signals and suppress interference between paired D2D and cellular links. We maximize the sum rate of D2D users and cellular users by jointly optimizing the resource reuse indicators, the transmit power and the RIS's passive beamforming. To solve the formulated non-convex problem, we first propose an efficient user-pairing scheme based on relative channel strength to determine the resource reuse indicators. Then, the transmit power and the RIS's passive beamforming are jointly optimized by an iterative algorithm, based on the techniques of alternating optimization, successive convex approximation, Lagrangian dual transform and quadratic transform. Numerical results show that the proposed design outperforms the traditional D2D network without RIS.**

***Index Terms*—Device-to-device communication, reconfigurable intelligent surfaces, passive beamforming, power allocation, iterative algorithm.**

I. Introduction

Device-to-device (D2D) communication underlaying cellular networks, which allows a device to communicate with its nearby device over the licensed cellular bandwidth, is recognized as a promising technology in future networks due to its advantages such as high spectrum efficiency, high energy efficiency (EE) and low transmission delay [1]. Interference management is the most important challenge for underlaying D2D communication. The D2D link and the cellular link operating in the same licensed band interfere with each other severely [2], and the interference needs to be carefully suppressed via efficient interference management [3] and resource allocation [4].

Recently, reconfigurable intelligent surfaces (RIS) have emerged as a new and revolutionary technology to achieve spectrum-, energy- and cost-efficient wireless networks [5]. Specifically, RIS consist of a large number of passive low-cost reflecting elements, each of which can adjust the phase and amplitude of the incident electromagnetic wave and reflect it passively [6]. Thus, RIS are able to enhance desired signals and suppress interference by designing the reflecting coefficient (including phase and amplitude) of each reflecting element. For instance, the weighted-sum rate of an RIS-aided multiuser multiple-input single-output downlink communication system was maximized in [7], by jointly optimizing the base station's (BS's) active beamforming and the RIS's passive beamforming (i.e., reflecting coefficients). The EE of an RIS-empowered downlink multi-user communication system was maximized in [8], by jointly optimizing the BS's transmit power and the RIS's passive beamforming.

RIS can be explored to enhance the strengths of desired signals for both D2D links and cellular links, and suppress the severe interference between each paired D2D link and cellular link. This motivates us to study RIS-empowered D2D communication underlaying a cellular network. Specifically, we formulate a problem to maximize the overall network sum rate, by jointly optimizing the resource reuse indicators (i.e., user pairing between D2D users and cellular users (CUs)), the transmit power and the RIS's passive beamforming, subject to the signal-to-interference-plus-noise ratio (SINR) constraints for both D2D links and cellular links. However, the problem is challenging to be solved optimally, since the user pairing and the resource allocation are closely coupled. Thus, we first propose an efficient relative-channel-strength based user-pairing scheme with low complexity. Under the obtained user pairing, an iterative algorithm based on alternating optimization is further proposed. The successive convex approximation technique is exploited to optimize the transmit power; while the Lagrangian dual transform and quadratic transform techniques are utilized to optimize the passive beamforming. The algorithm's convergency is proved and its complexity is analyzed. Numerical results show that the proposed design achieves significant sum-rate enhancement compared to underlaying D2D without RIS, and suffers from slight degradation compared to the best-achievable performance under ideal user pairing.

II. System Model

As shown in Fig. 1, we consider an RIS-empowered cellular network with underlay D2D, which consists of an RIS, $N \geq 1$ D2D transmitters (TXs) denoted as

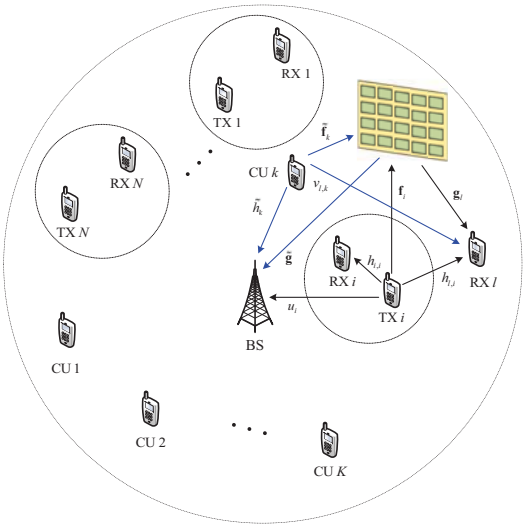

Fig. 1: An RIS-empowered underlaying D2D network.

TX $1,\ldots,$TX N, N D2D receivers (RXs) denoted as RX $1,\ldots,$RX N, $K \geq 1$ active CUs (i.e., cellular users) denoted as CU $1,\ldots,$CU K, and a cellular BS. The RIS has $M \geq 1$ reflecting elements, while each D2D TX, D2D RX, CU and the BS are equipped with a single antenna. A controller is attached to the RIS to control the reflecting coefficients and communicate with other network components through separate wireless links. We assume that the D2D links share the uplink (UL) spectrum of the cellular network, since the UL spectrum is typically under-utilized compared to the downlink spectrum. To alleviate interference, we consider that a D2D link shares at most one CU's spectrum resource, while the resource of a CU can be shared by at most one D2D link [3].

All channels are assumed to experience quasi-static flat-fading and be known. The channels from TX i $(1 \leq i \leq N)$ to RX l $(1 \leq l \leq N)$ and RIS are denoted by $h_{l,i} \in \mathcal{C}$ and $\mathbf{f}_i \in \mathcal{C}^{M\times 1}$, respectively. For notational clarity, we represent each channel related to the cellular network with a tilde. The channels from CU k $(1 \leq k \leq K)$ to BS and RIS are denoted by $\tilde{h}_k \in \mathcal{C}$ and $\tilde{\mathbf{f}}_k \in \mathcal{C}^{M\times 1}$, respectively; the channels from RIS to RX l and BS are denoted by $\mathbf{g}_l \in \mathcal{C}^{M\times 1}$ and $\tilde{\mathbf{g}} \in \mathcal{C}^{M\times 1}$, respectively; the interference channels from TX i to BS and from CU k to RX l are denoted by $u_i \in \mathcal{C}$ and $v_{l,k} \in \mathcal{C}$, respectively.

The transmitted signals from TX i and CU k are denoted as s_i and x_k, respectively, which follow independent circularly symmetric complex Gaussian (CSCG) distribution with zero mean and unit variance, i.e., $s_i \sim \mathcal{CN}(0,1)$, $x_k \sim \mathcal{CN}(0,1)$. Denote the index set of active D2D pairs as $\mathcal{D} \subseteq \{1,\ldots,N\}$. The corresponding SINR for RX n decoding s_n from D2D TX $n \in \mathcal{D}$ is

$$\gamma_n^d = \frac{P_n^d \left|\mathbf{g}_n^H \mathbf{\Phi} \mathbf{f}_n + h_{n,n}\right|^2}{\sum\limits_{k=1}^{K} \rho_{k,n} P_k^c \left|\mathbf{g}_n^H \mathbf{\Phi} \tilde{\mathbf{f}}_k + v_{n,k}\right|^2 + \sigma^2}, \tag{1}$$

where P_i^d and P_k^c are the transmit power of TX i and CU k, respectively; $\mathbf{\Phi} = \mathrm{diag}\{\alpha_1 e^{j\theta_1},\ldots,\alpha_M e^{j\theta_M}\}$ denotes the reflecting coefficient matrix, where $\alpha_m \in (0,1]$ and $\theta_m \in (0,2\pi]$; $\rho_{k,n}$ is the resource reuse indicator for cellular link k and D2D link n, $\rho_{k,n}=1$ when D2D link n reuses the resource of CU k, and $\rho_{k,n}=0$ otherwise; σ^2 is the power of additive white Gaussian noise (AWGN) at RX n.

The SINR for BS decoding x_k from CU k is

$$\gamma_k^c = \frac{P_k^c \left|\tilde{\mathbf{g}}^H \mathbf{\Phi} \tilde{\mathbf{f}}_k + \tilde{h}_k\right|^2}{\sum\limits_{i=1}^{N} \rho_{k,i} P_i^d \left|\tilde{\mathbf{g}}^H \mathbf{\Phi} \mathbf{f}_i + u_i\right|^2 + \sigma^2}, \tag{2}$$

where σ^2 is the power of AWGN at BS.

Hence, the overall network's sum rate in bps/Hz is

$$R(\boldsymbol{\rho}, \mathbf{p}, \mathbf{\Phi}) = \sum_{n\in\mathcal{D}} \log_2(1+\gamma_n^d) + \sum_{k=1}^{K} \log_2(1+\gamma_k^c), \tag{3}$$

where the length-(KN) resource reuse indicator vector $\boldsymbol{\rho} = [\rho_{1,1},\ldots,\rho_{1,N},\rho_{2,1},\ldots,\rho_{K,N}]^T$, and the length-$(K+N)$ power allocation vector $\mathbf{p} = \left[P_1^d,\ldots,P_N^d,P_1^c,\ldots,P_K^c\right]^T$.

III. PROBLEM FORMULATION

This paper aims to maximize the sum rate in (3), by jointly optimizing the resource reuse indicator vector $\boldsymbol{\rho}$, the transmit power vector $\mathbf{p}$ and the reflecting coefficients matrix $\mathbf{\Phi}$. The optimization problem is formulated as

$$\begin{aligned}
(\text{P1}): \quad & \max_{\boldsymbol{\rho},\mathbf{p},\mathbf{\Phi}} \quad R(\boldsymbol{\rho}, \mathbf{p}, \mathbf{\Phi}) && \text{(4a)}\\
& \text{s.t.} \quad \gamma_n^d \geq \gamma_{\min}^d, \quad n \in \mathcal{D} && \text{(4b)}\\
& \qquad \gamma_k^c \geq \gamma_{\min}^c, \quad 1 \leq k \leq K && \text{(4c)}\\
& \qquad \sum_{k=1}^{K} \rho_{k,n} \leq 1 && \text{(4d)}\\
& \qquad \sum_{n\in\mathcal{D}}^{N} \rho_{k,n} \leq 1 && \text{(4e)}\\
& \qquad 0 \leq P_n^d \leq P_{\max}^d && \text{(4f)}\\
& \qquad 0 \leq P_k^c \leq P_{\max}^c && \text{(4g)}\\
& \qquad 0 < \alpha_m \leq 1, \quad 1 \leq m \leq M && \text{(4h)}\\
& \qquad 0 < \theta_m \leq 2\pi, \quad 1 \leq m \leq M && \text{(4i)}
\end{aligned}$$

where (4b) and (4c) indicate the required minimum SINRs (i.e., quality-of-service) $\gamma_{\min}^d$ and $\gamma_{\min}^c$ for the D2D links and cellular links, respectively; (4d) ensures that a D2D link shares at most one CU's resource, while (4e) indicates that the resource of a CU can be shared by at most one D2D link; (4f) and (4g) are the maximum transmit power constraints on the TXs and CUs, respectively; (4h) and (4i) are the practical constraints on the reflecting coefficients.

Notice that (P1) is a non-convex problem. First, (P1) involves integer variables $\boldsymbol{\rho}$ and thus is NP-hard. Moreover, the objective function and the constraint functions of (4b)

and (4c) are non-concave with respect to the variables $\boldsymbol{\rho}$, $\mathbf{p}$ and $\boldsymbol{\Phi}$, and these variables are all coupled. There is no standard method to solve such a non-convex problem.

IV. Proposed Solution to (P1)

In order to solve (P1) effectively, we first propose an efficient user-pairing scheme to determine integer variables $\boldsymbol{\rho}$, then optimize $\mathbf{p}$ and $\boldsymbol{\Phi}$ in an iterative manner.

A. Relative-Channel-Strength based Pairing Scheme

Since the user-pairing design involves integer programming which is hard to solve, we propose a relative-channel-strength (RCS) based low-complexity pairing scheme to design the resource reuse indictors $\boldsymbol{\rho}$.

Notice that there are A_K^N different possible pairings denoted as a set $\Pi \triangleq \{\pi_1, \ldots, \pi_{A_K^N}\}$. Each possible pairing can be viewed as an index mapping denoted as $\pi_m : k \in \mathcal{U}_m \longrightarrow n \in \mathcal{D}_m$, for $m = 1, \ldots, A_N^K$, i.e., the mapping π_m maps each CU index $k \in \mathcal{U}_m \subset \{1, 2, \ldots, K\}$ to a D2D-link index $n \in \mathcal{D}_m \subset \mathcal{D}$. The RCS-based pairing scheme determines the pairing $\pi_{m^\star}$ by the following criterion

$$\pi_{m^\star} = \arg\max_{\pi_m \in \Pi} \sum_{k \in \mathcal{U}_m} \frac{|\tilde{h}_k|^2}{|v_{\pi_m(k),k}|^2}. \tag{5}$$

This heuristic pairing scheme chooses the pairing mapping which maximizes the sum of the ratios of each paired-CU-to-BS channel strength over the paired CU-to-RX interference channel strength. Clearly, this heuristic pairing scheme that requires only simple comparison features low complexity, but fortunately its resultant design only suffers from slight performance degradation compared to the design with ideal pairing achieved by exhaustive search, as numerically shown in Section V.

B. Algorithm for Solving (P1) with Given Pairing Design

After heuristic pairing, we apply the alternating optimization (AO) [9] algorithm to decouple the variables $\mathbf{p}$ and $\boldsymbol{\Phi}$. For given $\boldsymbol{\Phi}$, we optimize $\mathbf{p}$ based on the successive convex approximation (SCA) technique [10]. For given $\mathbf{p}$, we optimize $\boldsymbol{\Phi}$ based on the Lagrangian dual transform and quadratic transform techniques [11].

1) Optimizing Transmit Power Vector $\mathbf{p}$*:* In each iteration j, for given reflecting coefficient matrix $\boldsymbol{\Phi}$, the transmit power vector $\mathbf{p}$ can be optimized by solving

$$\text{(P1.1)}: \quad \max_{\mathbf{p}} \quad R(\mathbf{p}) \tag{6a}$$

$$\text{s.t.} \quad \text{(4b), (4c), (4f), (4g).} \tag{6b}$$

The objective function of (P1.1) is non-convex due to its $\mathbf{p}$-dependence. We exploit the SCA technique to solve (P1.1). Specifically, we need to find a concave lower bound to approximate the objective function. Since any convex function can be lower bounded by its first-order Taylor expansion at any point, we obtain the following concave lower bound R^{lb} at the point $\mathbf{p}^{(j)}$

$$\begin{aligned} R \geq \sum_{n \in \mathcal{D}} \Bigg[& \log_2\left(\sum_{k=1}^{K} P_n^d Q_{n,n}^{(j)} + A_1\right) - \log_2\left(A_1^{(j)}\right) \\ & - \frac{1}{A_1^{(j)}} \sum_{k=1}^{K} \rho_{k,n} \widetilde{Q}_{n,k}^{(j)} \left(P_k^c - P_k^{c(j)}\right) \Bigg] \\ & + \sum_{k=1}^{K} \Bigg[\log_2\left(P_k^c \widetilde{Q}_k^{(j)} + A_2\right) - \log_2\left(A_2^{(j)}\right) \\ & - \frac{1}{A_2^{(j)}} \sum_{i=1}^{N} \rho_{k,i} Q_i^{(j)} \left(P_i^d - P_i^{d(j)}\right) \Bigg] = R^{\text{lb}}, \end{aligned} \tag{7}$$

where $Q_{n,n} = |\mathbf{g}_n^H \boldsymbol{\Phi} \mathbf{f}_n + h_{n,n}|^2$, $\widetilde{Q}_{n,k} = |\mathbf{g}_n^H \boldsymbol{\Phi} \tilde{\mathbf{f}}_k + v_{n,k}|^2$, $\widetilde{Q}_k = |\tilde{\mathbf{g}}^H \boldsymbol{\Phi} \tilde{\mathbf{f}}_k + \tilde{h}_k|^2$, $Q_i = |\tilde{\mathbf{g}}^H \boldsymbol{\Phi} \mathbf{f}_i + u_i|^2$, $A_1 = \sum_{k=1}^{K} \rho_{k,n} P_k^c \widetilde{Q}_{n,k}^{(j)} + \sigma^2$ and $A_2 = \sum_{i=1}^{N} \rho_{k,i} P_i^d Q_i^{(j)} + \sigma^2$.

With given $\mathbf{p}^{(j)}$ and R^{lb}, (P1.1) is approximated as

$$\text{(P1.2)}: \max_{\mathbf{p}} \quad R^{\text{lb}} \tag{8a}$$

$$\text{s.t.} \quad \text{(4b), (4c), (4f), (4g).} \tag{8b}$$

(P1.2) is convex and can be solved by CVX [12].

2) Optimizing Reflecting Coefficient Matrix $\boldsymbol{\Phi}$*:* In each iteration j, for given transmit power vector $\mathbf{p}$, the reflecting coefficient matrix $\boldsymbol{\Phi}$ can be optimized by solving

$$\text{(P2.1)}: \max_{\boldsymbol{\Phi}} \quad R(\boldsymbol{\Phi}) \tag{9a}$$

$$\text{s.t.} \quad \text{(4b), (4c), (4h), (4i).} \tag{9b}$$

We tackle the logarithm in the objective function via the Lagrangian dual transform technique. Introducing auxiliary variables $\boldsymbol{\eta}_n^d = [\eta_1^d, \ldots, \eta_N^d]^T$ and $\boldsymbol{\eta}_k^c = [\eta_1^c, \ldots, \eta_K^c]^T$, the new objective function can be equivalently expressed as

$$\begin{aligned} R_a(\boldsymbol{\Phi}) = & \max_{\boldsymbol{\eta}_n^d} \left(\sum_{n \in \mathcal{D}} \log\left(1+\eta_n^d\right) - \sum_{n \in \mathcal{D}} \eta_n^d + \sum_{n \in \mathcal{D}} \frac{(1+\eta_n^d)\gamma_n^d}{1+\gamma_n^d} \right) \\ & + \max_{\boldsymbol{\eta}_k^c} \left(\sum_{k=1}^{K} \log(1+\eta_k^c) - \sum_{k=1}^{K} \eta_k^c + \sum_{k=1}^{K} \frac{(1+\eta_k^c)\gamma_k^c}{1+\gamma_k^c} \right). \end{aligned} \tag{10}$$

It is easy to validate that the optimal values of $\boldsymbol{\eta}_{\text{opt}}^{d(j)}$ and $\boldsymbol{\eta}_{\text{opt}}^{c(j)}$ are $\boldsymbol{\gamma}^{d(j)}$ and $\boldsymbol{\gamma}^{c(j)}$, respectively. We define $\boldsymbol{\theta}^H \boldsymbol{\omega}_{n,n} = \mathbf{g}_n^H \boldsymbol{\Phi} \mathbf{f}_n$, $\boldsymbol{\theta}^H \tilde{\boldsymbol{\omega}}_{n,k} = \mathbf{g}_n^H \boldsymbol{\Phi} \tilde{\mathbf{f}}_k$, $\boldsymbol{\theta}^H \tilde{\boldsymbol{\omega}}_k = \tilde{\mathbf{g}}^H \boldsymbol{\Phi} \tilde{\mathbf{f}}_k$ and $\boldsymbol{\theta}^H \boldsymbol{\omega}_i = \tilde{\mathbf{g}}^H \boldsymbol{\Phi} \mathbf{f}_i$. From (1) and (2), optimizing the reflecting coefficient $\boldsymbol{\Phi}$ can be equivalently transformed into optimizing $\boldsymbol{\theta}$ in the following objective function

$$\begin{aligned} R_a(\boldsymbol{\theta}) = & \sum_{n \in \mathcal{D}} \frac{\left(1+\eta_{\text{opt},n}^{d(j)}\right) P_n^{d(j)} Q_{n,n}^w}{P_n^{d(j)} Q_{n,n}^w + \sum_{k=1}^{K} \rho_{k,n} P_k^{c(j)} \widetilde{Q}_{n,k}^w + \sigma^2} \\ & + \sum_{k=1}^{K} \frac{\left(1+\eta_{\text{opt},k}^{c(j)}\right) P_k^{c(j)} \widetilde{Q}_k^w}{P_k^{c(j)} \widetilde{Q}_k^w + \sum_{i=1}^{N} \rho_{k,i} P_i^{d(j)} Q_i^w + \sigma^2}, \end{aligned} \tag{11}$$

where $Q_{n,n}^w = |\boldsymbol{\theta}^H \boldsymbol{\omega}_{n,n} + h_{n,n}|^2$, $\widetilde{Q}_{n,k}^w = |\boldsymbol{\theta}^H \widetilde{\boldsymbol{\omega}}_{n,k} + v_{n,k}|^2$, $\widetilde{Q}_k^w = |\boldsymbol{\theta}^H \widetilde{\boldsymbol{\omega}}_k + \tilde{h}_k|^2$ and $Q_i^w = |\boldsymbol{\theta}^H \boldsymbol{\omega}_i + u_i|^2$.

Then, utilizing the quadratic transform method proposed in [11], we introduce an auxiliary variable $\mathbf{y} = [y_1^d, \ldots, y_N^d, y_1^c, \ldots, y_K^c]^T$, transforming (11) to

$$\begin{aligned} R_b(\boldsymbol{\theta}, \mathbf{y}) = & \\ & \sum_{n\in\mathcal{D}} \left[2\sqrt{\left(1+\eta_{\text{opt},n}^{d(j)}\right) P_n^{d(j)}} \text{Re}\left\{ y_n^{d*} \boldsymbol{\theta}^H \boldsymbol{\omega}_{n,n} + y_n^{d*} h_{n,n} \right\} \right. \\ & \left. - |y_n^d|^2 \left(P_n^{d(j)} Q_{n,n}^w + \sum_{k=1}^K \rho_{k,n} P_k^{c(j)} \widetilde{Q}_{n,k}^w + \sigma^2 \right) \right] \\ & + \sum_{k=1}^K \left[2\sqrt{(1+\eta_{\text{opt},k}^{c(j)}) P_k^{c(j)}} \text{Re}\left\{ y_k^{c*} \boldsymbol{\theta}^H \widetilde{\boldsymbol{\omega}}_k + y_k^{c*} \tilde{h}_k \right\} \right. \\ & \left. - |y_k^c|^2 \left(P_k^{c(j)} \widetilde{Q}_k^w + \sum_{i=1}^N \rho_{k,i} P_i^{d(j)} Q_i^w + \sigma^2 \right) \right]. \end{aligned} \tag{12}$$

We first optimize $\mathbf{y}$ with fixed $\boldsymbol{\theta}$, then optimize $\boldsymbol{\theta}$ with fixed $\mathbf{y}$. It can be easily confirmed that $R_b(\boldsymbol{\theta}, \mathbf{y})$ is a concave differentiable function over $\mathbf{y}$ with fixed $\boldsymbol{\theta}$, so the optimal solution of $\mathbf{y}$ can be obtained by setting $\partial R_b(\boldsymbol{\theta}^{(j)}, \mathbf{y})/\partial \mathbf{y} = 0$. The optimal value of $\mathbf{y}$ is given by

$$y_{\text{opt},n}^{d(j)} = \frac{\sqrt{\left(1+\eta_{\text{opt},n}^{d(j)}\right) P_n^{d(j)}} \left[\boldsymbol{\theta}^{H(j)} \boldsymbol{\omega}_{n,n} + h_{n,n} \right]}{P_n^{d(j)} Q_{n,n}^w + \sum_{k=1}^K \rho_{k,n} P_k^{c(j)} \widetilde{Q}_{n,k}^w + \sigma^2} \tag{13}$$

$$y_{\text{opt},n}^{c(j)} = \frac{\sqrt{\left(1+\eta_{\text{opt},k}^{c(j)}\right) P_k^{c(j)}} \left[\boldsymbol{\theta}^{H(j)} \widetilde{\boldsymbol{\omega}}_k + \tilde{h}_k \right]}{P_k^{c(j)} \widetilde{Q}_k^w + \sum_{i=1}^N \rho_{k,i} P_i^{d(j)} Q_i^w + \sigma^2}. \tag{14}$$

Then, we replace y_n^d and y_k^c with $y_{\text{opt},n}^{d(j)}$ and $y_{\text{opt},k}^{c(j)}$, respectively. Denote $\mathbf{B}_{1n} = P_n^{d(j)} \boldsymbol{\omega}_{n,n} \boldsymbol{\omega}_{n,n}^H$, $\mathbf{B}_{2n} = \sum_{k=1}^K \rho_{k,n} P_k^{c(j)} \widetilde{\boldsymbol{\omega}}_{n,k} \widetilde{\boldsymbol{\omega}}_{n,k}^H$, $\mathbf{B}_{1b} = P_k^{c(j)} \widetilde{\boldsymbol{\omega}}_k \widetilde{\boldsymbol{\omega}}_k^H$, $\mathbf{B}_{2b} = \sum_{i=1}^N \rho_{k,i} P_i^{d(j)} \boldsymbol{\omega}_i \boldsymbol{\omega}_i^H$, $\mathbf{e}_{1n} = P_n^{d(j)} h_{n,n}^* \boldsymbol{\omega}_{n,n}$, $\mathbf{e}_{2n} = \sum_{k=1}^K \rho_{k,n} P_k^{c(j)} v_{n,k}^* \widetilde{\boldsymbol{\omega}}_{n,k}$, $\mathbf{e}_{1b} = P_k^{c(j)} \tilde{h}_k^* \widetilde{\boldsymbol{\omega}}_k$ and $\mathbf{e}_{2b} = \sum_{i=1}^N \rho_{k,i} P_i^{d(j)} u_i^* \boldsymbol{\omega}_i$. Optimizing $\boldsymbol{\theta}$ for given $\mathbf{y}$, the objective function is transformed as follows

$$R_b(\boldsymbol{\theta}, \mathbf{y}) = -\boldsymbol{\theta}^H \mathbf{B}_1 \boldsymbol{\theta} + 2\text{Re}\left(\boldsymbol{\theta}^H \mathbf{e}_1\right) + C_1, \tag{15}$$

where C_1 is a constant, the matrix $\mathbf{B}_1$ and vector $\mathbf{e}_1$ are

$$\mathbf{B}_1 = \sum_{n\in\mathcal{D}} \left| y_{\text{opt},n}^{d(j)} \right|^2 \mathbf{B}_n + \sum_{k=1}^K \left| y_{\text{opt},k}^{c(j)} \right|^2 \mathbf{B}_b \tag{16}$$

$$\begin{aligned} \mathbf{e}_1 = & \sum_{n\in\mathcal{D}} \left[\sqrt{\left(1+\eta_{\text{opt},n}^{d(j)}\right) P_n^{d(j)}} \left(y_{\text{opt},n}^{d(j)} \right)^* \boldsymbol{\omega}_{n,n} - \left| y_{\text{opt},n}^{d(j)} \right|^2 \mathbf{e}_n \right] \\ & + \sum_{k=1}^K \left[\sqrt{\left(1+\eta_{\text{opt},k}^{c(j)}\right) P_k^{c(j)}} \left(y_{\text{opt},k}^{c(j)} \right)^* \widetilde{\boldsymbol{\omega}}_k - \left| y_{\text{opt},k}^{c(j)} \right|^2 \mathbf{e}_b \right], \end{aligned} \tag{17}$$

with $\mathbf{B}_n = \mathbf{B}_{1n} + \mathbf{B}_{2n}$, $\mathbf{B}_b = \mathbf{B}_{1b} + \mathbf{B}_{2b}$, $\mathbf{e}_n = \mathbf{e}_{1n} + \mathbf{e}_{2n}$, and $\mathbf{e}_b = \mathbf{e}_{1b} + \mathbf{e}_{2b}$.

Algorithm 1 Proposed algorithm for solving (P1)

Step 1: Initialize $\mathbf{p}^{\{0\}}$, $\boldsymbol{\Phi}^{\{0\}}$, a small threshold constant $\epsilon = 10^{-4}$. Let $j = 0$.
Step 2: Exploting RCS-based pairing scheme to determine the resource resue indictor vector $\boldsymbol{\rho}$.
repeat
  Step 3: Solve problem (P1.2) for given $\boldsymbol{\Phi}^{(j)}$, and obtain the optimal solution as $\mathbf{p}^{\{j+1\}}$.
  Step 4: Solve problem (P2.2) for given $\mathbf{p}^{\{j+1\}}$, and obtain the optimal solution as $\boldsymbol{\Phi}^{\{j+1\}}$:
  Step 5: Update iteration index $j = j + 1$.
until The increase of objective value is smaller than ϵ
Step 6: Return the suboptimal solution $\boldsymbol{\rho}^\star = \boldsymbol{\rho}^{\{j-1\}}$, $\mathbf{p}^\star = \mathbf{p}^{\{j-1\}}$ and $\boldsymbol{\Phi}^\star = \boldsymbol{\Phi}^{\{j-1\}}$

Similarly, leveraging the quadratic transform method, the constraints (4b) and (4c) can be transformed into

$$f_d(\boldsymbol{\theta}) = -\boldsymbol{\theta}^H \mathbf{B}_2 \boldsymbol{\theta} + 2\text{Re}\left(\boldsymbol{\theta}^H \mathbf{e}_2\right) + C_2 \geq \gamma_{\min}^d, \tag{18}$$

$$f_c(\boldsymbol{\theta}) = -\boldsymbol{\theta}^H \mathbf{B}_3 \boldsymbol{\theta} + 2\text{Re}\left(\boldsymbol{\theta}^H \mathbf{e}_3\right) + C_3 \geq \gamma_{\min}^c, \tag{19}$$

where $x_d = \frac{\sqrt{P_n^{d(j)}} \left(\boldsymbol{\theta}^{H(j)} \boldsymbol{\omega}_{n,n} + h_{n,n} \right)}{\sum_{k=1}^K \rho_{k,n} P_k^{c(j)} \widetilde{Q}_{n,k}^w + \sigma^2}$, $\mathbf{B}_2 = |x_d|^2 \mathbf{B}_{2n}, \mathbf{e}_2 = \sqrt{P_n^{d(j)}} x_d^* \boldsymbol{\omega}_{n,n} - |x_d|^2 \mathbf{e}_{2n}$, $C_2 = 2\sqrt{P_n^{d(j)}} \text{Re}\left\{ x_d^* h_{n,n} \right\} - |x_d|^2 (\sum_{k=1}^K \rho_{k,n} P_k^{c(j)} |v_{n,k}|^2 + \sigma^2)$; $x_c = \frac{\sqrt{P_k^{c(j)}} \left(\boldsymbol{\theta}^{H(j)} \widetilde{\boldsymbol{\omega}}_k + \tilde{h}_k \right)}{\sum_{i=1}^N \rho_{k,i} P_i^{d(j)} Q_{b,i}^w + \sigma^2}, \mathbf{B}_3 = |x_c|^2 \mathbf{B}_{2b}$, $\mathbf{e}_3 = \sqrt{P_k^{c(j)}} x_c^* \widetilde{\boldsymbol{\omega}}_k - |x_c|^2 \mathbf{e}_{2b}$, and $C_3 = 2\sqrt{P_k^{c(j)}} \text{Re}\left\{ x_c^* \tilde{h}_k \right\} - |x_c|^2 \left(\sum_{i=1}^N \rho_{k,i} P_i^{d(j)} |u_i|^2 + \sigma^2 \right)$.

Hence, (P2.1) is transformed into the following problem

$$\text{(P2.2)}: \max_{\boldsymbol{\theta}} -\boldsymbol{\theta}^H \mathbf{B}_1 \boldsymbol{\theta} + 2\text{Re}\left(\boldsymbol{\theta}^H \mathbf{e}_1\right) + C_1 \tag{20}$$

$$\text{s.t.} \quad (18), (19), (4h), (4i). \tag{21}$$

The resulting (P2.2) is a quadratic constrained quadratic programming (QCQP) problem. Thus, (P2.2) can also be effectively solved by standard methods.

C. Overall Algorithm

Theorem 1. *Algorithm 1 is guaranteed to converge.* [1]

Proof: First, in Step 3, since the optimal solution $\mathbf{p}^{\{j+1\}}$ is obtained for given $\boldsymbol{\Phi}^{\{j\}}$, we have the following inequality on the sum rate

$$R\left(\mathbf{p}^{\{j\}}, \boldsymbol{\Phi}^{\{j\}}\right) \overset{(a)}{=} R^{\text{lb}}\left(\mathbf{p}^{\{j\}}, \boldsymbol{\Phi}^{\{j\}}\right)$$

[1]Notice that AO algorithm can generally converge to a stationary point [9], but AO-based Algorithm 1 can not guarantee to converge to a stationary point due to the applied techniques of SCA, Lagrangian dual transform and quadratic transform.

$$\overset{(b)}{\leq} R^{\text{lb}}\left(\mathbf{p}^{\{j+1\}}, \mathbf{\Phi}^{\{j\}}\right)$$
$$\overset{(c)}{=} R\left(\mathbf{p}^{\{j+1\}}, \mathbf{\Phi}^{\{j\}}\right), \quad (22)$$

where (a) and (c) hold since the Taylor expansion in (7) is tight at given local points $\mathbf{p}^{\{j\}}$ and $\mathbf{p}^{\{j+1\}}$, respectively, and (b) holds since $\mathbf{p}^{\{j+1\}}$ is the optimal solution to (P1.2).

Second, in Step 4, since $\mathbf{\Phi}^{\{j+1\}}$ is the optimal solution to (P2.2), we can obtain the following inequality

$$R\left(\mathbf{p}^{\{j+1\}}, \mathbf{\Phi}^{\{j\}}\right) \leq R\left(\mathbf{p}^{\{j+1\}}, \mathbf{\Phi}^{\{j+1\}}\right). \quad (23)$$

From (22) and (23), it's straightforward that

$$R\left(\mathbf{p}^{\{j\}}, \mathbf{\Phi}^{\{j\}}\right) \leq R\left(\mathbf{p}^{\{j+1\}}, \mathbf{\Phi}^{\{j+1\}}\right). \quad (24)$$

Since the objective value is non-decreasing after each iteration and is upper bounded by some positive constant, the overall Algorithm 1 is guaranteed to converge. ■

Problems (P1.2) and (P2.2) are alteratively solved in each outer-layer AO iteration. Specifically, (P1.2) can be solved in $(N+K)\log_2(N+K)$ operations by the extended water-filling algorithm [13], while (P2.2) is a convex QCQP which can be solved by using interior point methods with complexity $\mathcal{O}(M^{3.5})$ [14]. Hence, the complexity of Algorithm 1 is $\mathcal{O}\left(I_{\text{ite}}[(N+K)\log_2(N+K)+M^{3.5}]\right)$, where I_{ite} denotes the number of outer-layer AO iterations.

V. NUMERICAL RESULTS

We assume that $h_{l,i}$, u_i, $\tilde{h}_k$ and $v_{l,k}$ are independently Rayleigh fading distributed, while $\mathbf{f}_i$, $\tilde{\mathbf{f}}_k$, $\mathbf{g}_l$ and $\tilde{\mathbf{g}}$ follow independent Rician fading distribution, i.e.,

$$\mathbf{f}_i = \sqrt{\frac{K_1}{K_1+1}}\mathbf{f}_{\text{L},i} + \sqrt{\frac{1}{K_1+1}}\mathbf{f}_{N,i}, \quad (25)$$

where K_1 is the Rician factor of $\mathbf{f}_i$, $\mathbf{f}_{\text{L},i}$ is the line of sight (LoS) component, and $\mathbf{f}_{\text{N},i}$ is the non-LoS (NLOS) component each element of which follows distribution $\mathcal{CN}(0,\beta_i)$, where β_i is the large-scale pathloss. Set $K_1 = 10$. Similarly, $\tilde{\mathbf{f}}_k$, $\mathbf{g}_l$ and $\tilde{\mathbf{g}}$ are generated in the same way as $\mathbf{f}_i$ with Rician factors $K_2 = K_3 = K_4 = 10$.

We assume that the CUs are uniformly distributed in the cellular cell with radius $R = 250$ meters (m). We adopt the clustered distribution model in [3] for D2D users, i.e., the clusters are randomly located in the cell, and each D2D link is uniformly distributed in one cluster with radius $r = 60$ m. We set $K = 4$ and $N = 2$. The RIS is located between two D2D clusters. Using the above method, the locations of CUs and D2D users are generated by one realization, and then fixed in all the simulations. The coordinates of CU 1, CU 2, CU 3 and CU 4 are (38, 54), (87, 92), (112, 136) and (155, 89), respectively; the coordinates of TX 1 and RX 1 are (97, 28), (144, 52), respectively; the coordinates of TX 2 and RX 2 are (44, 103), (52, 154), respectively; the coordinate of RIS is (100, 0). The large-scale path losses β's from TXs and CUs to RXs are $10^{-3}d^{-4}$, from TXs and CU to BS are $10^{-3}d^{-3.8}$, the other pass-losses of RIS-related channels are $10^{-3}d^{-2.2}$ [3] [7] [15], where d is the distance in meters. We set $M = 200$, $P_{\max} = P^d_{\max} = P^c_{\max} = 24$dBm , $R^d_{\min} = R^c_{\min} = \log_2(1+\gamma^d_{\min}) = 0.3$ bps/Hz, and $\sigma^2 = -114$ dBm [16]. The simulation results are based on 1000 channel realizations.

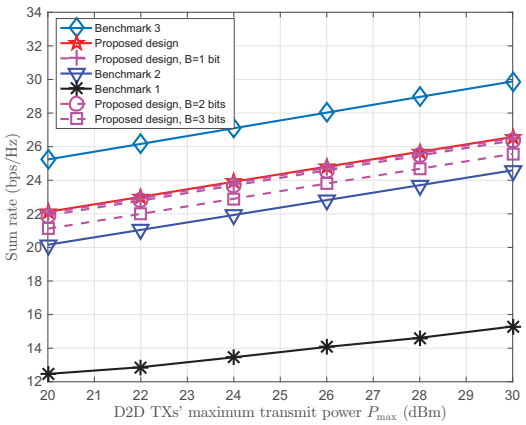

Fig. 2: Sum rate versus maximum transmit power $P^d_{\max}$.

For comparison, we consider the following three benchmarks, i.e., (1) underlaying D2D without RIS, (2) proposed design with random reflecting coefficients, (3) RIS-empowered D2D with ideal user pairing. For the first benchmark, we consider the traditional RIS-empowered D2D underlaying a cellular network without RIS. We maximize the sum rate by jointly optimizing the resource reuse indicator $\boldsymbol{\rho}$ and the transmit power vector $\mathbf{p}$. We use the solving algorithm in [3] for this problem, and omit the details herein. For the second benchmark, we maximize the sum rate by jointly optimizing $\boldsymbol{\rho}$ and $\mathbf{p}$. All reflecting elements are set with random phase and maximal amplitude. For the third benchmark, we exhaustively search over A^N_K possible user-pairings, and jointly optimize $\mathbf{p}$ as well as $\mathbf{\Phi}$ under each pairing. This benchmark gives an achievable upper-bound sum-rate performance.

Fig. 2 plots the sum rate versus D2D TX's maximum transmit power $P_{\max}$. The proposed design achieves significant sum rate gain compared to the first benchmark. For instance, the sum rate of the proposed RCS-based design is 77.42% and 73.8% higher than that of the first benchmark when $P_{\max}$ is 20 and 30 dBm, respectively. In addition, the proposed design outperforms the second benchmark without optimizing $\mathbf{\Phi}$, which shows the benefit of passive beamforming optimization. Moreover, compared to the third benchmark based on exhaustive search, the proposed design has slight degradation of performance, but obviously outperforms this benchmark in terms of computational complexity. The proposed design solves the joint-resource-allocation optimization problem only once, while the third benchmark needs to solve such problem for A^N_K times under all possible pairings, resulting into

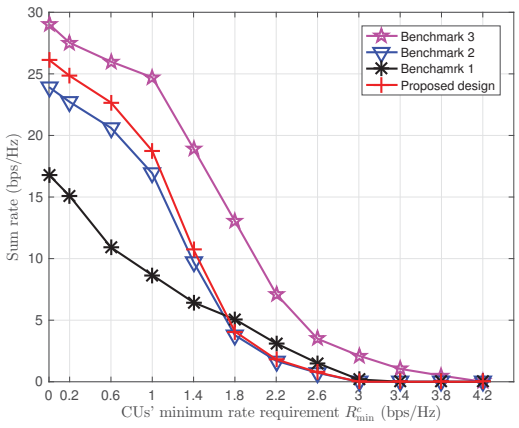

Fig. 3: Sum rate versus CUs' rate requirement $R^c_{\min}$.

unaffordable complexity especially for large numbers of D2D and cellular links. Furthermore, the sum rate increases as the phase-shift quantization bit B increase. In particular, the 2-bit phase shifter can obtain sufficiently high performance gain with a slight performance degradation compared to the ideal case of continuous phase shifters.

Fig. 3 plots the sum rate versus the CUs' minimum rate requirement $R^c_{\min}$. The sum rate decreases as $R^c_{\min}$ increases, which reveals the rate tradeoff between the D2D links and the cellular links. Compared to the first benchmark, the proposed design achieves significant sum-rate gain by introducing the RIS for $R^c_{\min} \leq 1.5$ bps/Hz. For $R^c_{\min} \geq 1.5$ bps/Hz, the first benchmark achieves higher sum rate as compared to the proposed design. The reason is that both the pairing scheme and the benefits introduced by the RIS affect the sum rate performance. When $R^c_{\min}$ is relatively small, the proposed design with a suboptimal pairing scheme is able to obtain a feasible solution, the performance enhancement comes from the well-designed RIS; in contrast, when $R^c_{\min}$ is too large, the problem is not likely to be solved under a suboptimal pairing scheme, which results into worse performance of the proposed design as compared to the first benchmark with ideal pairing. Also, the proposed design outperforms the second benchmark, and suffers from slight sum-rate performance degradation compared to the third benchmark.

VI. Conclusion

This paper has maximized the overall sum rate of an RIS-empowered underlaying D2D communication network. First, an efficient relative-channel-strength based user-pairing scheme with low complexity is proposed to determine the resource reuse indicators. Then, the transmit power and the passive beamforming are optimized by utilizing the proposed alternating-optimization based iterative algorithm. Numerical results show that the proposed design achieves significant performance enhancement compared to underlaying D2D network without RIS, and suffers from slight performance degradation compared to RIS-empowered underlying D2D with ideal user-pairing. This work can be extended to other scenarios such as multi-antenna BS/users and multiple RISs.

Acknowledgment

This work of Gang Yang, Yating liao, and Ying-Chang Liang was supported by the National Natural Science Foundation of China (Grant No. 61631005, 62071093 and U1801261), the National Key Research and Development Program of China under Grant 2018YFB1801105 , the Fundamental Research Funds for the Central Universities under Grant ZYGX2019Z022, and the Programme of Introducing Talents of Discipline to Universities under Grant B20064. This work of Olav Tirkkonen was supported by Academy of Finland under Grant 319484.

References

[1] A. Asadi, Q. Wang, and V. Mancuso, "A survey on device-to-device communication in cellular networks," *IEEE Commun. Sur. & Tut.*, vol. 16, no. 4, pp. 1801–1819, 2014.

[2] Y.-C. Liang, *Dynamic Spectrum Management: From Cognitive Radio to Blockchain and Artificial Intelligence*, ser. Signals and Communication Technology. Singapore: Springer, 2020.

[3] D. Feng, L. Lu, Y. Yuan-Wu, G. Y. Li, G. Feng, and S. Li, "Device-to-device communications underlaying cellular networks," *IEEE Trans. Commun.*, vol. 61, no. 8, pp. 3541–3551, 2013.

[4] C. Yu, K. Doppler, C. B. Ribeiro, and O. Tirkkonen, "Resource sharing optimization for device-to-device communication underlaying cellular networks," *IEEE Trans. Wireless Commun.*, vol. 10, no. 8, pp. 2752–2763, 2011.

[5] Y.-C. Liang, R. Long, Q. Zhang, J. Chen, H. V. Cheng, and H. Guo, "Large intelligent surface/antennas (LISA): Making reflective radios smart," *J. Commun. Inf. Netw.*, vol. 4, no. 2, pp. 40–50, Jun. 2019.

[6] G. Yang, X. Xu, Y.-C. Liang, and M. D. Renzo, "Reconfigurable intelligent surface assisted non-orthogonal multiple access," *IEEE Trans. Wireless Commun.*, Jan. 2021, DOI: 10.1109/TWC.2020.3047632.

[7] H. Guo, Y.-C. Liang, J. Chen, and E. G. Larsson, "Weighted sum-rate maximization for reconfigurable intelligent surface aided wireless networks," *IEEE Tran. Wireless Commun.*, vol. 19, no. 5, pp. 3064–3076, 2020.

[8] C. Huang, A. Zappone, G. C. Alexandropoulos, M. Debbah, and C. Yuen, "Reconfigurable intelligent surfaces for energy efficiency in wireless communication," *IEEE Trans. Wireless Commun.*, vol. 18, no. 8, pp. 4157–4170, 2019.

[9] M. Hong, M. Razaviyayn, Z.-Q. Luo, and J.-S. Pang, "A unified algorithmic framework for block-structured optimization involving big data: With applications in machine learning and signal processing," *IEEE Signal Processing Mag.*, vol. 33, no. 1, pp. 57–77, 2015.

[10] A. Beck, A. Ben-Tal, and L. Tetruashvili, "A sequential parametric convex approximation method with applications to nonconvex truss topology design problems," *J. Global Opt.*, vol. 47, no. 1, pp. 29–51, 2010.

[11] K. Shen and W. Yu, "Fractional programming for communication systemsłpart I: power control and beamforming," *IEEE Trans. Signal Processing*, vol. 66, no. 10, pp. 2616–2630, 2018.

[12] M. Grant, S. Boyd, and Y. Ye, "CVX: Matlab software for disciplined convex programming," 2008.

[13] Y.-F. Liu and Y.-H. Dai, "On the complexity of joint subcarrier and power allocation for multi-user OFDMA systems," *IEEE Trans. Signal Processing*, vol. 62, no. 3, pp. 583–596, 2013.

[14] A. Hassanien, S. A. Vorobyov, and K. M. Wong, "Robust adaptive beamforming using sequential quadratic programming: An iterative solution to the mismatch problem," *IEEE Signal Processing Lett.*, vol. 15, pp. 733–736, 2008.

[15] G. Yang, Y.-C. Liang, R. Zhang, and Y. Pei, "Modulation in the air: Backscatter communication over ambient OFDM carrier," *IEEE Trans. Commun.*, vol. 66, no. 3, pp. 1219–1233, Mar. 2018.

[16] G. Yang, Q. Zhang, and Y.-C. Liang, "Cooperative ambient backscatter communications for green Internet-of-Things," *IEEE Internet of Things J.*, vol. 5, no. 2, pp. 1116–1130, Apr. 2018.